The Adsorption of Dyes onto Chitin in Fixed Bed Columns and Batch Adsorbers

G. McKAY, H. S. BLAIR, and J. R. GARDNER, *Department of Chemical Engineering, The Queen's University of Belfast, Belfast BT9 5DL, Northern Ireland*

Synopsis

Chitin has the ability to adsorb substantial quantities of dyestuffs from aqueous solutions. Consequently, it may be a useful adsorbent for effluent treatment from textile mills. The design procedures for batch and continuous fixed bed adsorption columns have been investigated for four dyestuffs, namely, CI Acid Blue 25 (Telon Blue ANL, Bayer), CI Acid Blue 158 (Neolan Blue 29, Ciba Geigy) CI Mordant Yellow 5 (Eriochrome Flavine A, Ciba Geigy), and CI Dirert Red 84 (Solophenyl Brown 3RL, Ciba Geigy). The main fixed bed system variables studied are bed height, dye flow rate, and chitin particle size, and these effects have been incorporated into a simplified design model.

INTRODUCTION

The ability of chitin to adsorb large amounts of various dyestuffs has been reported.[1] The kinetics of these processes have been developed for agitated batch adsorbers based on external mass transfer[2] and intraparticle diffusion processes.[3]

It is important to consider the methods of contacting the solid adsorbent and the wastewater when applying the adsorption system to large-scale treatment. Two major classes of contacting system exist, namely, batch type processes and bed or columnar systems. The bed type processes may be fixed bed or fluidized bed systems; only fixed bed adsorbers will be considered in this paper.

Batch type process are usually limited to the treatment of small volumes of effluent, but small adsorbent particle sizes may be used hence large external surface areas are available for mass transfer. Fixed bed systems, however, would sustain high pressure drop losses if fine adsorbent particles were used, but they have an advantage because adsorption depends on the concentration of solute in the solution being treated. The adsorbent is continuously in contact with fresh solution; hence the concentration in the solution in contact with a given layer of adsorbent in a column is relatively constant. Conversely, the concentration of solute in contact with a given quantity of adsorbent is continuously changing due to the solute being adsorbed.

The aim of the present work is to predict the performance of batch adsorbers using experimental data and present results for the fixed bed adsorption of dyestuffs onto chitin.

Journal of Applied Polymer Science, Vol. 29, 1499–1514 (1984)
 CCC 0021-8995/84/051499-16$04.00

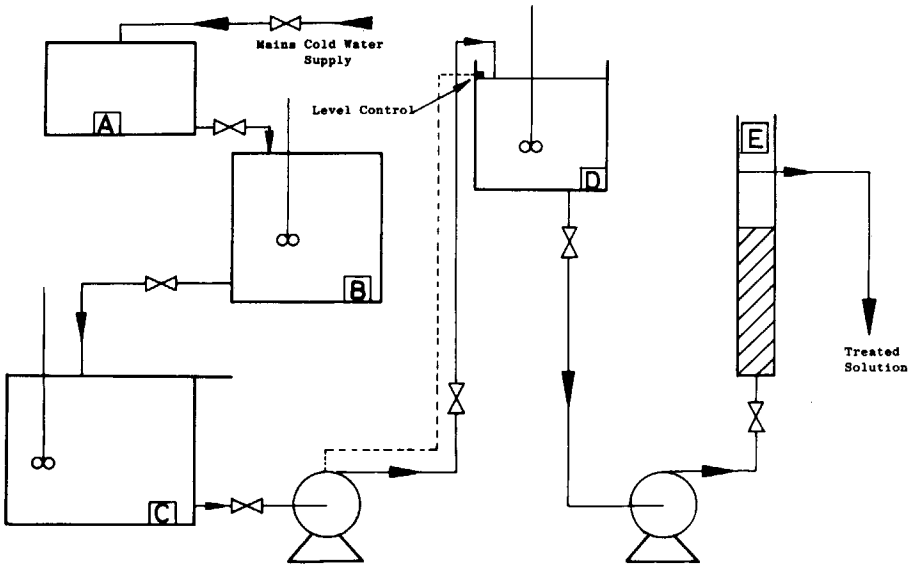

Fig. 1. Apparatus for column adsorption studies.

EXPERIMENTAL

Details pertaining to the dyestuffs, chitin and batch adsorption studies have been presented previously.[1,2]

Continuous column operation by means of fixed beds was studied using perspex columns of 4.5 cm internal diameter and 55 cm length, installed in a vertical position (see Fig. 1). The column had a wire mesh placed at the dye entrance point with approx. 3 cm of graded glass beads (smallest next to bed) placed on top. This arrangement ensured that the dye solution was distributed uniformly in the column, (see Fig. 2).

Sub-a-seals were used as sample ports for syringe sampling and were placed at regular intervals up the length of the column. A fixed mass of constant particle size chitin was placed in the column, and the sides were gently tapped until a fixed bed height was established. To prevent disturbance of the bed by high flow rates, another mesh/glass bead arrangement was used at the top of the bed. The columns were then connected into the continuous flow apparatus represented in Figure 1. In this diagram vessel A was calibrated mains cold water, storage container (30 dm^3); vessels B and C were 60-dm^3 solution storage containers with stirrers to give adequate mixing. An accurately weighed amount of dye, in the form of a 5 cm^3 dye slurry, was washed into B using the contents of A. C was the constant concentration dye reservoir from which the dye solution was pumped to D, a level and temperature controlled, agitated, overhead glass vessel of 20 dm^3 capacity. The dye solution was then pumped from D to the column(s) E.

The flow rates in the columns were measured by rotameters and finely controlled by jubilee clips. For each run, the rotameters were calibrated by measuring their output volume over a fixed time and then they were set for a fixed flow rate. The rotameters used were supplied by G.E.C.—Elliot Process In-

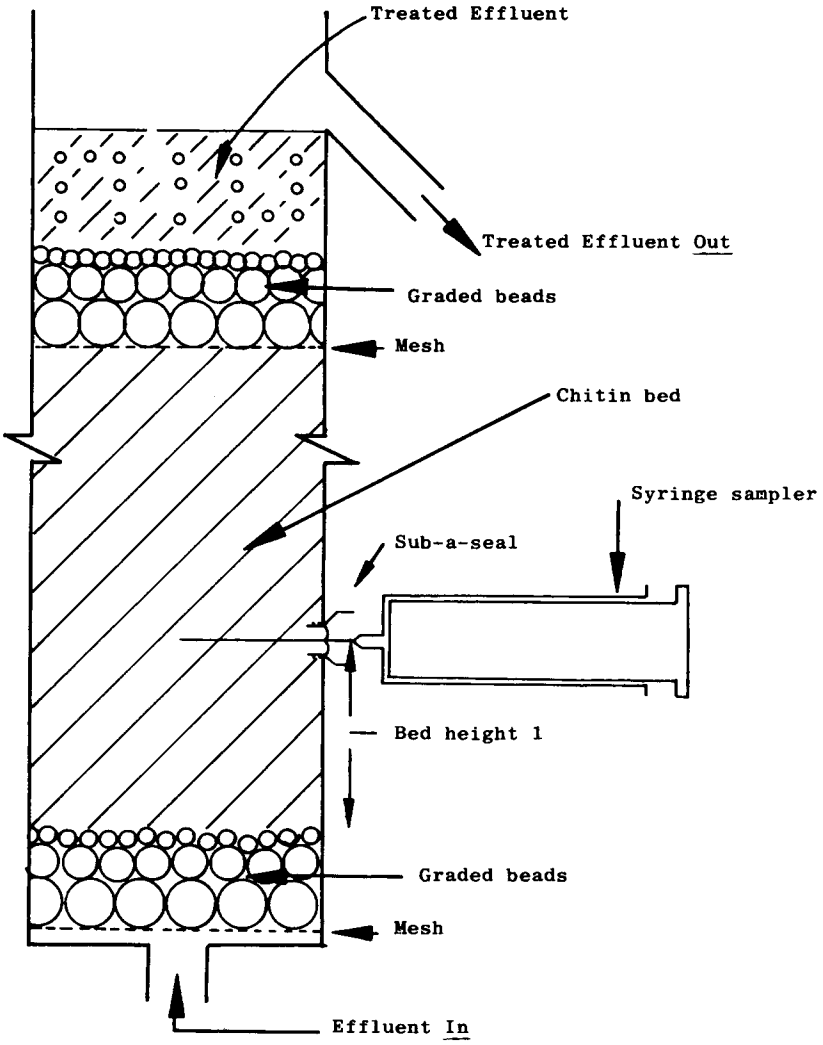

Fig. 2. Schematic representation of column showing first bed height.

struments Ltd., England. Sampling (2.5 cm^3) was carried out at three points in the apparatus at regular time intervals. C_0 was monitored by sampling vessel D; $C_{t,h}$ was determined by sampling at the bed height sample ports, and C_{dis} (= C_t for top of bed) was sampled at the column exit point.

RESULTS AND DISCUSSION

Single-Stage Batch Adsorption

The dye solution to be treated and the chitin were agitated in a treatment tank for a sufficient period of time to enable the system to approach equilibrium. The slurry was then filtered to separate the solid phase and adsorbed dye from the

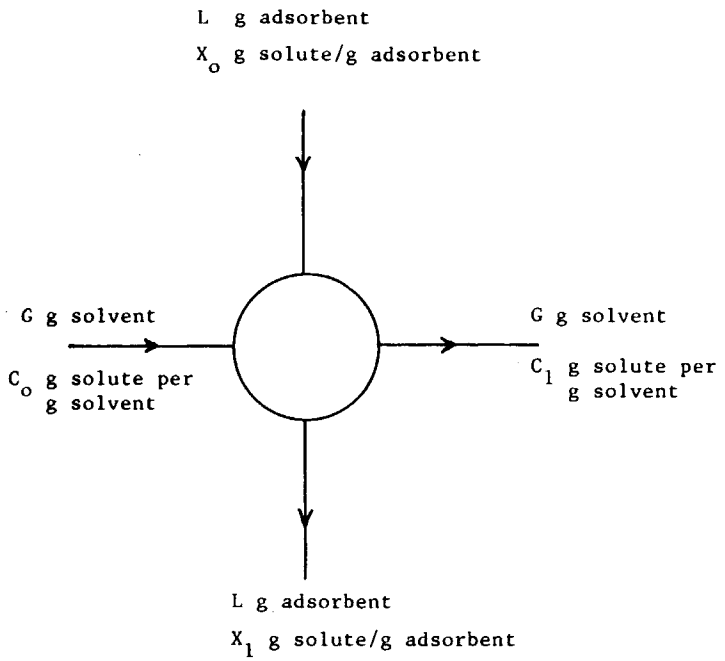

Fig. 3. Single stage batch adsorption.

liquid. If required, batch contacting equipment can be made multistage by providing additional tanks and filters.

A schematic diagram of the process is shown in Figure 3. The solution to be treated contains G dm^3 of solvent, in this case water, and the liquid phase dye concentration is to be reduced from C_0 to C_1 mg dye·dm^{-3} water. The chitin adsorbent is added, L_g, and the solute phase dye concentration increases from X_0 to X_1 mg dye·g^{-1} chitin. If fresh chitin is used, then $X_0 = 0$.

The mass balance is given by Eq. (1) relating the dye removed from the liquid to that accumulated by chitin:

$$G(C_0 - C_1) = L(X_1 - X_0) = LX_1 \tag{1}$$

Equation (1) may be solved by substituting for X_1 from the Freundlich equation or the Langmuir equation. These isotherm equations have been presented previously,[1] and the isotherm parameters were determined and tabulated. Rearrangement of eq. (1) yields eqs. (2) and (3) for the Freundlich and Langmuir isotherms, respectively:

$$\frac{L}{G} = \frac{C_0 - C_1}{(C_1/P)^{1/n}} \tag{2}$$

$$\frac{L}{G} = (C_0 - C_1)\frac{(1 + BC_1)}{K_L C_1} \tag{3}$$

Optimum dye uptake for a particular system is achieved as $C_1 \rightarrow C_\infty$. Equations (2) and (3) permit analytical calculation of the adsorbent/solution ratio for a given change in solution concentration from C_0 to C_1. A series of plots is

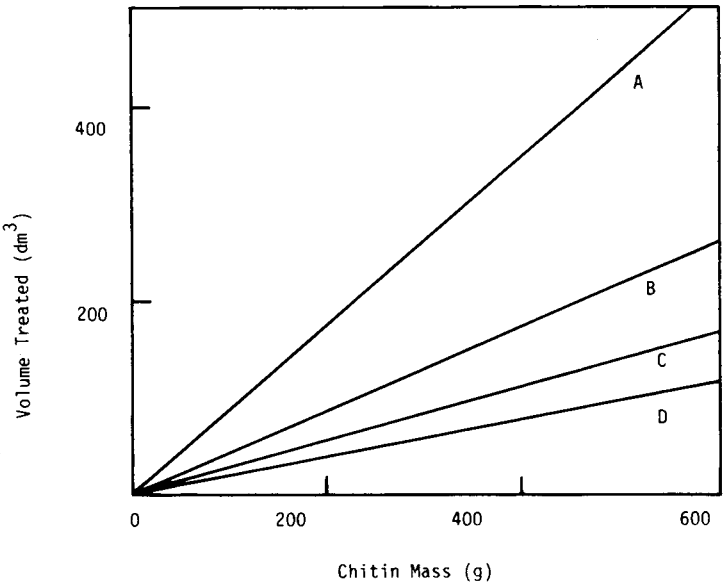

Fig. 4. Volume of dye removed (dm^3) against mass of chitin for a single stage batch process at various extents of removal: (A) $C_1/C_0 = 0.8$; (B) $C_1/C_0 = 0.6$; (C) $C_1/C_0 = 0.4$; (D) $C_1/C_0 = 0.2$.

shown in Figure 4 for various C_1/C_0 ratios for the adsorption of CI Acid Blue 25 onto chitin (500–710 μm) at 20°C. The isotherms are based on the data in Paper I,[1] and Figure 4 was evaluated assuming the Langmuir data and an initial dye concentration of 200 mg·dm^{-3}. The results may be used to predict the design of single stage batch adsorbers with limited accuracy since the problems associated with scale-up have to be considered.

A similar set of data are represented in Figure 5 for all four dyestuffs. An initial dye solution concentration of 200 mg·dm^{-3} is assumed, and 50% removal, that is, $C_1/C_0 = 0.5$, is required. The appropriate Langmuir parameters were used in eq. (3) to evaluate the data for a particle size range 500–710 μm. The results illustrate how much of each dyestuff can be removed using a certain amount of chitin for 50% breakthrough. These design lines are easy to construct for any specified breakthrough point.

The major disadvantages of batch adsorption operations are: (i) the time required to achieve equilibrium is quite long; (ii) plant items include an agitated tank and a filter press or rotary filters for semicontinuous operation, which are quite expensive items; (iii) additional hold-up time for the filtration process.

Fixed Bed Column Studies

The majority of commercial adsorption systems utilize the principle of fixed bed systems. The concept of fixed bed adsorbers is the establishment of a breakthrough curve, which passes through the column until it leaves the column, at which stage the adsorbent will be spent and in need of regeneration. At this stage the concentration of dye in the effluent will be the same as that at the influent, namely, C_0. The liquid phase dye concentration across the breakthrough

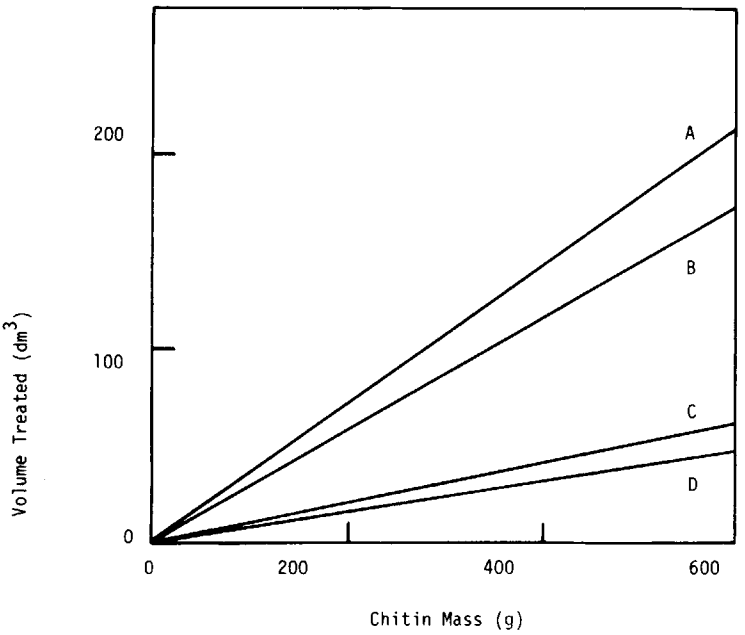

Fig. 5. Volume of dye removed (dm^3) against mass of chitin for a single stage batch process at 50% breakthrough for four dyestuffs: (A) CI Acid Blue 25; (B) CI Acid Blue 158; (C) CI Mordant Yellow 5; (D) CI Direct Red 84.

curve changes from C_0 to zero, and the solid phase dye concentration changes from an equilibrium value X_1 to zero. Thus there is a dynamic equilibrium established in fixed bed columns with fresh dye solution continuously coming into contact with fresh adsorbent.

In fixed bed adsorption systems a finite time is required for the process to reach equilibrium. The main design criterion is to predict how long the adsorbent

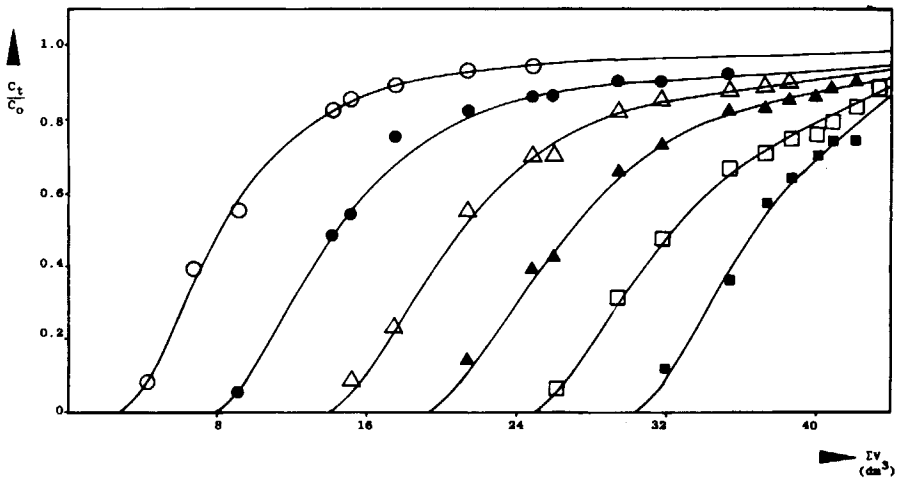

Fig. 6. Breakthrough curves for AB 25 at 40 $cm^3 \cdot min^{-1}$ (855 μ chitin): (⊙) 6 cm; (●) 11 cm; (△) 16 cm; (▲) 21 cm; (⊡) 26 cm; (■) 30 cm.

TABLE I
Fixed Bed Column Studies[a]

Dye	d_p (μm)	F ($cm^3 \cdot min^{-1}$)	W (g)	T (°C)	C_0 ($mg \cdot dm^{-3}$)
CI Acid Blue 25	855	23, 38, 82, 95, 120	100	18.2	100
CI Acid Blue 25	200, 302, 407, 605	95	100	18.2	100
CI Acid Blue 158	605	56, 65, 75, 91, 120	100	18.2	100
CI Acid Blue 158	200, 302, 427, 855	65	100	18.2	100
CI Mordant Yellow 5	855	42, 58, 80, 102, 117	100	18.2	100
CI Mordant Yellow 5	302, 427, 605	80	100	18.2	100
CI Direct Red 84	605	40, 64, 75, 95, 120	100	18.2	100
CI Direct Red 84	302	65	100	18.2	100

[a] Key: The runs underlined were selected to study the effect of flow rate.

material will be able to sustain removing a specified amount of impurity from solution before replacement or regeneration is needed; this period of time is called the service time of the bed. All existing models are based on determining breakthrough curves for specific systems, and Figure 6 shows a series of breakthrough curves at different bed heights for the adsorption of CI Acid Blue 25 (C_0 = 100 $mg \cdot dm^{-3}$) onto chitin (d_p = 710–1000 μm). A dye flow rate of 40 $cm^3 \cdot min^{-1}$ was adopted and the mass of chitin in the column was 100 g. Details of experimental parameters for all the column runs undertaken are listed in Table I.

Figure 7 shows a series of breakthrough curves for Telon Blue onto chitin under similar experimental conditions to those used in Figure 6 except for a higher dye flow rate, namely, 95 $cm^3 \cdot min^{-1}$. At the lower flow rate the curves are steeper, indicative of the longer adsorbent/solute contact time at the lower flow rate, enabling a more rapid approach to equilibrium. The overall adsorption capacity at each bed height for the two flowrates is similar.

Figures 8 and 9 show the influence of chitin particle size for the adsorption of CI Mordant Yellow 5 at constant dye flow rate. The curves for the smaller

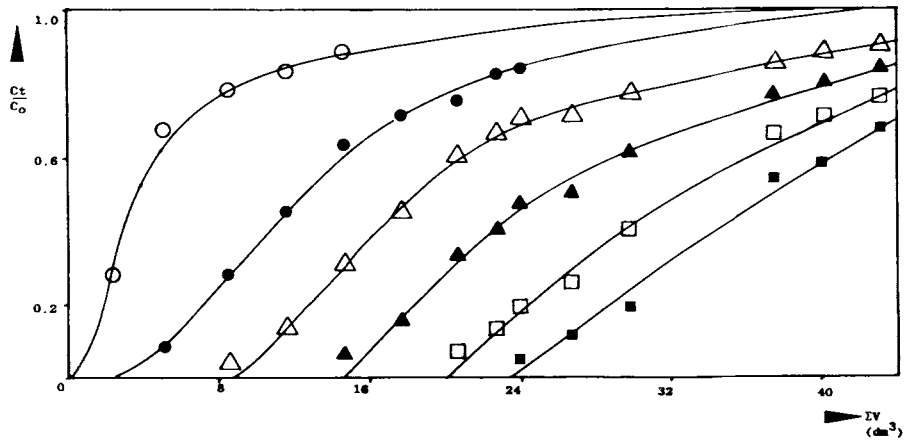

Fig. 7. Breakthrough curves for AB 25 at 95 $cm^3 \cdot min^{-1}$ (855 μ chitin): (⊙) 5 cm; (●) 10 cm; (△) 15 cm; (▲) 20 cm; (⊡) 25 cm; (■) 29.5 cm.

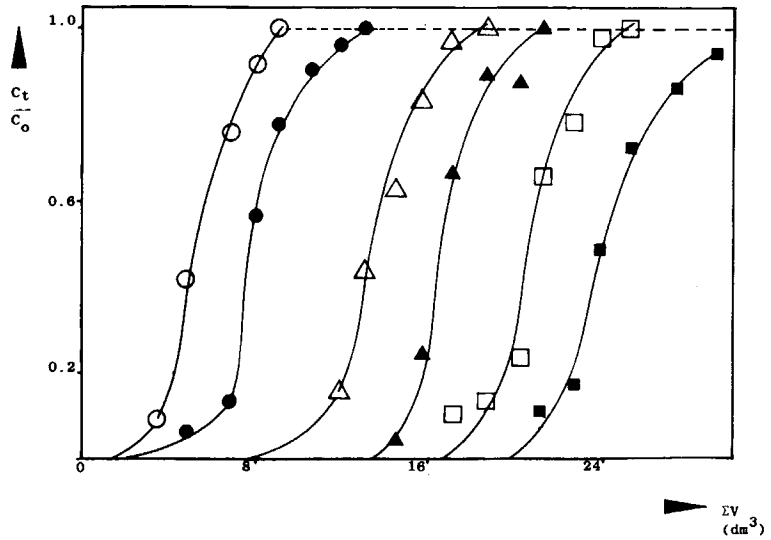

Fig. 8. Breakthrough curves for MY 5 (427 μ chitin): (⊙) 6 cm; (●) 11 cm; (△) 16 cm; (▲) 21 cm; (⊡) 26 cm; (■) 34 cm; F = 80 cm^3·min^{-1}.

particle diameter range are very steep compared to the higher range, indicating much more rapid adsorption. This effect is again expected due to the larger external surface area available for adsorption onto small particles and also the mean intraparticle diffusion paths are shorter.

For an ideal deep fixed-bed with a single adsorbate in dilute solution the service time of a column has been expressed[4,5] as a function of operational parameters. A simpler approach to fixed bed adsorbers has been proposed,[6–8] to correlate the

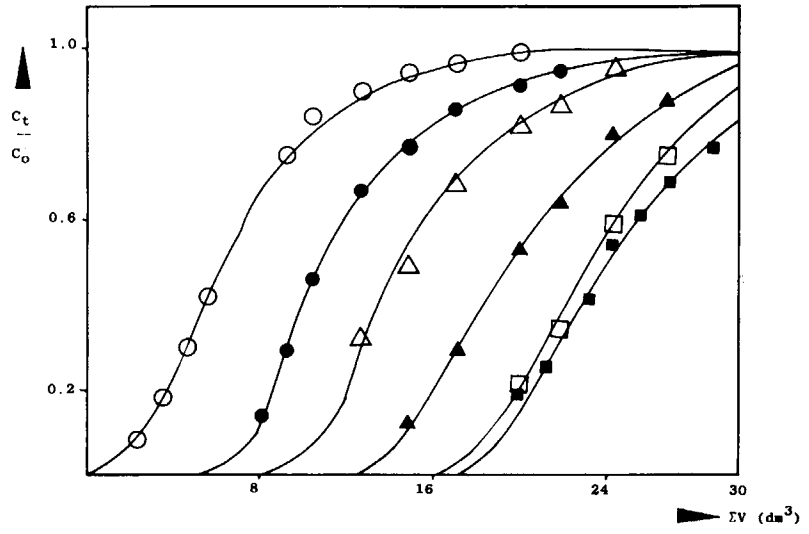

Fig. 9. Breakthrough curves for MY 5 (855 μ chitin): (⊙) 5.5 cm; (●) 10.5 cm; (△) 15.5 cm; (▲) 20.5 cm; (⊡) 25.5 cm; (■) 27.5 cm; F = 80 cm^3·min^{-1}.

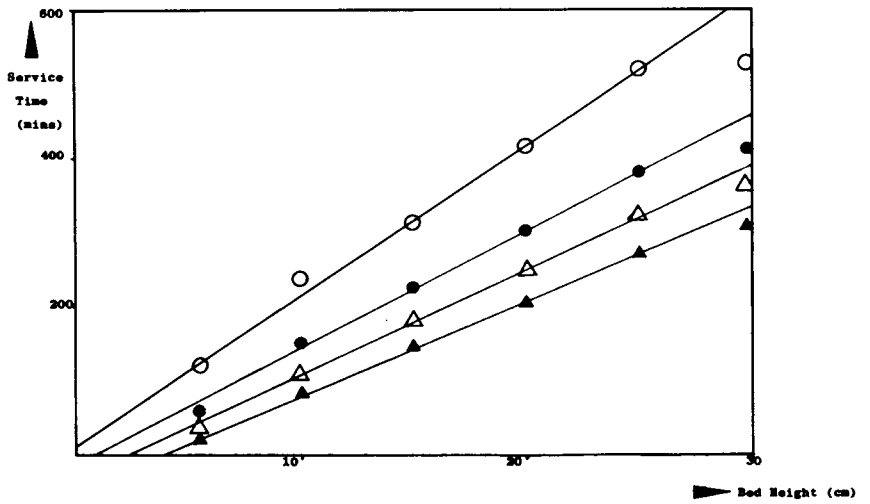

Fig. 10. BDST plots at 20%, 40%, 60%, and 80% breakthrough for AB 25: (⊙) 80%; (●) 60%; (△) 40%; (▲) 20%; PS 855 μ.

service time t with the process variables. The model is termed the bed depth service time (BDST) model and states that the service time t of a column is given by the following equation:

$$t = \frac{N_0}{C_0 u}\left[L_b - \frac{u}{k_a N_0}\ln\left(\frac{C_0}{C_t} - 1\right)\right] \tag{4}$$

The function

$$\frac{u}{k_a N_0}\ln\left(\frac{C_0}{C_t} - 1\right)$$

is the bed depth over which adsorption takes place. By plotting service time t against bed depth L_b from experimental data, N_0 can be evaluated from the slope of the graph, and k_a is obtained from the intercept at $t = 0$. The slope of the line predicted by eq. (4) is the time in minutes required to exhaust 0.01 m of chitin bed under test conditions, i.e., it is the time needed for the wavefront to move through 1 cm of chitin. The reciprocal of the slope is the rate at which the chitin bed is spent, and multiplying this value by the adsorbent's apparent bulk density gives an estimate of the chitin usage rate to continuously produce an acceptable product.

The intercept from the plot of eq. (4) is the critical bed depth L_m defined as the minimum bed depth for obtaining satisfactory effluent at time zero under the test operating conditions. The intercept of the ordinate is a measure of the adsorption rate and represents the time required for the adsorption wavefront to pass through the critical bed depth.

In the application of the BDST model certain boundary conditions should be noted: (i) when $C_t = C_0$ at $t = 0$ the log term of eq. (4) reduces to zero; (ii) when $C_0/C_t = 2$, at 50% breakthrough, the log term of eq. (4) reduces to zero. This approach enables the relative efficiencies of the chitin for the adsorption for all four dyes to be compared in the form of the volume of dye solution treated at 50%

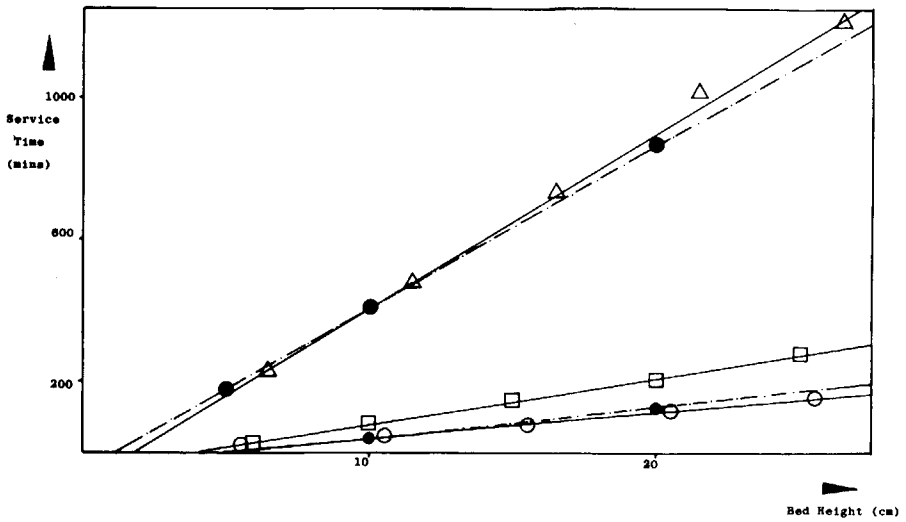

Fig. 11. AB 25 BDST predicted plots for 25 and 120 $cm^3 \cdot min^{-1}$ at 20% breakthrough using 80 $cm^3 \cdot min^{-1}$ as the control ($cm^3 \cdot min^{-1}$): (△) 25 (experimental); (-·-●-·-) 25 (predicted); (⊡) 80 (experimental—control); (⊙) 120 (experimental); (-·-●-·-) 120 (predicted); PS 855 μ.

breakthrough vs. bed height of the columns. The results are shown in Figure 10 using a chitin particle size range of 500–710 μm and a dye flow rate of 90 $cm^3 \cdot min^{-1}$ for three dyestuffs. The Eriochrome Flavine A column was operated at 78 $cm^3 \cdot min^{-1}$, and, in Figure 10, this appears alongside the BDST theoretically predicted line for 90 $cm^3 \cdot min^{-1}$. The method of predicting such operating lines is described in the next section using eq. (5). The figure shows a plot of volume dye treated instead of service time, but the two parameters are directly proportional. It is clear that the chitin adsorption of the three dyes CI Acid Blue 25, CI Acid Blue 158, and CI Mordant Yellow 5 are very similar, and it demonstrates that the fixed bed adsorption of CI Direct Red 84 is not a viable process. In fact, analyzing all the column data on the basis of service time indicates that the service time of the CI Direct Red 84 columns rarely exceeded 2 h compared to between 12 and 30 h for the other three dyes.

The BDST equation is easier to use in its simplified form:

$$t = a'L_b + b \tag{5}$$

where

$$a = \frac{N_0}{C_0 u} \quad \text{and} \quad b = \frac{u}{k_a N_0}\left(\ln \frac{C_0}{C_t} - 1\right)$$

Effect of Bed Height

Equation (5) is the equation of a straight line relating service time to bed depth and may be used directly to test the BDST model. Figure 11 shows how this relationship was confirmed for the adsorption of CI Acid Blue 25 onto chitin at different percentage breakthrough values for various bed depths. The data fit

TABLE II
BDST Data for CI Acid Blue 25 Removal with Chitin (710–1000 μm) and a Dye Flow Rate of 80 $cm^3 \cdot min^{-1}$

Bed depth (cm)	Service time at breakthrough for percentage removals (min)			
	20%	40%	60%	80%
6	20	40	52	122
10	83	110	151	240
15	145	180	225	316
20	202	250	305	420
25	275	330	390	525
29.5	305	370	415	605

the BDST model well and the equations of the four lines are given for a flow rate of 80 $cm^3 \cdot min^{-1}$:

$$20\%\ t = 12.8L_b - 50 \tag{6}$$

$$40\%\ t = 13.9L_b - 38 \tag{7}$$

$$60\%\ t = 15.9L_b - 14 \tag{8}$$

$$80\%\ t = 21.3L_b + 15 \tag{9}$$

The BDST data are given in Table II in terms of bed depth L_b and service time t for CI Acid Blue 25 (C_0 = 100 $mg \cdot dm^{-3}$) onto chitin (710–1000 μm) for a flow rate of 80 $cm^3 \cdot min^{-1}$.

Effect of Dye Velocity

In the design of fixed bed adsorption columns contact time is the most significant variable, and therefore bed depth and dye flow rate are the major design

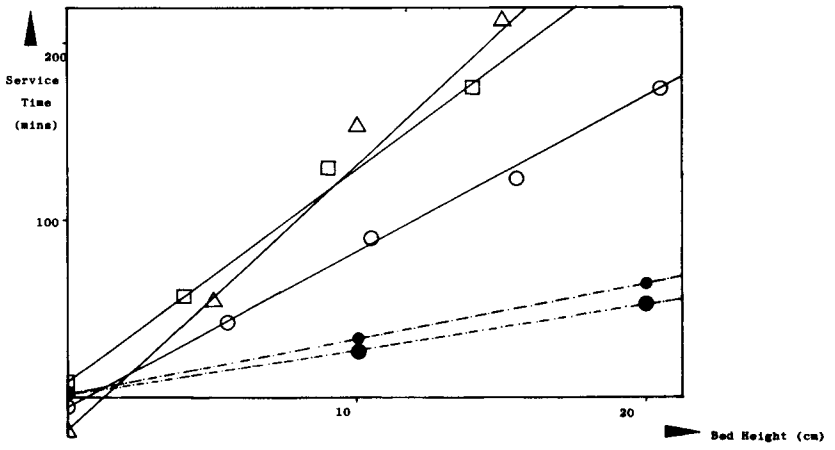

Fig. 12. AB 25 BDST predicted plots for 200 and 855 μ at 60% breakthrough using a 427 μ control: (△) 855 μ (experimental); (⊡) 427 μ (experimental—control); (⊙) 200 μ (experimental); (-·-●-·-) 855 μ (predicted); (-·-●-·-) 200 μ (predicted); F = 95 $cm^3 \cdot min^{-1}$.

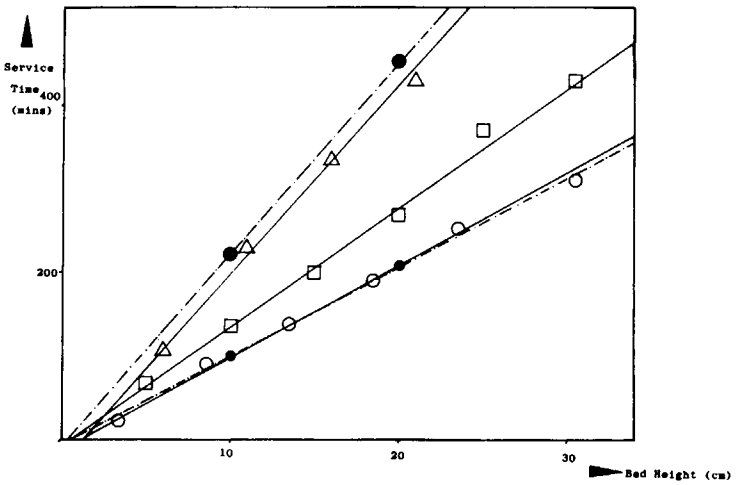

Fig. 13. AB 158 BDST predicted plots for 60 and 120 $cm^3 \cdot min^{-1}$ at 60% breakthrough using 90 $cm^3 \cdot min^{-1}$ as the control ($cm^3 \cdot min^{-1}$): (△) 60 (experimental); (-·-●-·-) 60 (predicted); (⊡) 90 (experimental—control); (⊙) 120 (experimental); (-·-●-·-) 120 (predicted); PS 605 μ.

parameters. A wide range of flowrates were investigated for the four dyestuffs and are listed in Table I. The BDST plots of the experimental points are shown in Figures 12 and 13, respectively, for Telon Blue and Neolan Blue 2G, respectively. The regression lines for the experimental data are shown by the solid lines on the figures. The BDST design equation can be tested using these data, and eq. (5) can be represented as

$$t = (\phi/u)L_o + b \tag{10}$$

where ϕ, in eq. (10), becomes N_0/C_0.

The linear velocity u is proportional to the flow rate of dye since the cross-sectional column area was constant in all experiments. Therefore, ratios of u are equal to flow rate ratios, i.e.,

$$\frac{u_2}{u_1} = \frac{F_2}{F_1} \tag{11}$$

where F_2 and F_1 are dye flow rates ($cm^3 \cdot min^{-1}$).

For each dyestuff one particular flowrate was selected from Table I and used to obtain the constants a and b in the BDST equation. These control flow rates are underlined in Table I. Having established a theoretical equation, it is possible to test the BDST model as shown in Figures 12 and 13. The intercept on the abscissa is the critical bed depth for obtaining satisfactory effluent at time zero under the test operating conditions. The theoretical equations at other values than the control flowrate are obtained by multiplying the constant ϕ by the ratio of the new and original rates; thus

$$t = (u_2/u_1)\phi L_b + b \tag{12}$$

where u_1 is the control flowrate and u_2 represents the various other flow rates

TABLE III
Comparison of Experimental and Theoretical BDST Constants a and b for CI Acid Blue 25 and CI Acid Blue 158

Percentage breakthrough	Flow rate	Exptl a	Predicted a	Exptl b	Predicted b
		CI Acid Blue 25			
20	25	50	47	−90	−50
40	25	53	49	−70	−38
60	25	56	57	−15	−14
80	25	66	72	−85	+15
20	120	7.4	8.8	−34	−50
40	120	8.0	9.5	−14	−38
60	120	8.5	11	−6	−14
80	120	13	14	+10	+15
		CI Acid Blue 158			
20	50	20	18	−64	−32
40	50	21	22	−52	−52
60	50	23	23	−28	−8
80	50	25	28	+10	+24
20	120	8	8.6	−25	−32
40	120	9.6	10	−28	−52
60	120	11	11	−16	−8
80	120	9	13	+26	+24

being tested. The form of eq. (12) shows that constant a is flow rate dependent and can be represented by

$$a = (u_2/u_1)a' \tag{13}$$

There is good agreement between experimental and theoretical plots in Figures 12 and 13, indicating that the effect of dye flow rate is explained by the BDST

TABLE IV
Comparison of Experimental and Theoretical BDST Constants a and b for CI Mordant Yellow 5 and CI Direct Red 84

Percentage breakthrough	Flow rate	Exptl a	Predicted a	Exptl b	Predicted b
		CI Mordant Yellow 5			
20	40	21	19	−24	−6
40	40	19	20	+42	+8
60	40	18	22	+96	+28
80	40	18	22	+152	+70
20	120	5.2	6.9	−8	−6
40	120	6.1	7.3	+1	+8
60	120	6.5	7.7	+13	+28
80	120	7.4	7.9	+32	+70
		CI Direct Red 84			
20	40	1.7	1.4	−15	−4.8
40	40	2.3	1.7	−17	−4.5
60	40	3.7	2.6	−20	−5.0
20	120	0.4	0.5	−5.3	−4.8
40	120	0.8	0.6	−8.9	−4.5
60	120	1.1	0.9	−8.0	−5.0

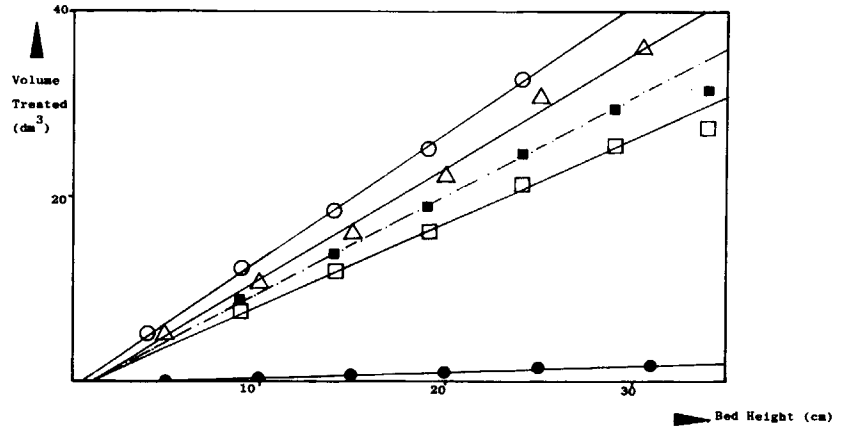

Fig. 14. Volume treated vs. bed height (BDVT) for the four dyes (605 μ; 90 $cm^3 \cdot min^{-1}$): (⊙) AB 25; (△) AB 158; (-·-■-·-) MY 5 (predicted for 90 $cm^3 \cdot min^{-1}$ by BDVT method); (□) MY 5 (78 $cm^3 \cdot min^{-1}$); (●) DR 84.

model. A comparison of the constants a and b in eq. (5) is presented in Tables III and IV. The agreement between experimental data and theoretically predicted data may be seen.

Effect of Particle Size

The particle size effect was difficult to interpret. The conventional lines for the BDST plots are shown in Figure 14 by the solidus lines. This represents a set of data based on eq. (5) for the adsorption of Telon Blue for three chitin particle size ranges and a constant flowrate of 95 $cm^3 \cdot min^{-1}$ at 60% breakthrough. This form of interpretation assumes the particle, internal and external surface, is completely saturated with dye. For the two larger particle sizes, the data are of a similar order of magnitude; however, the lower chitin particle size shows some deviation. Consequently, another model equation was tested, namely, that the uptake is dependent on expernal particle surface. For this case, the BDST equation is modified to

$$t = (d_1/d_2)^2(aL_b + b) \tag{14}$$

where d_1 and d_2 are the arithmetic mean chitin particle diameters and d_2 is taken as the control value. This equation is plotted on Figure 14 for two particle size ranges, and the theoretical lines are well outside the experimental data. Consequently, the theory of complete particle saturation seems more satisfactory, and any deviation is possibly due to the inability of large dye molecules to completely penetrate all the internal pores of the particle.

In order to obtain a comparison of the results for the four dyes, the amount of dye treated to 50% breakthrough, using a constant dye flow rate, was determined for a series of chitin particle sizes. The results are given in Table V, and the volume of dye treated for any one system is almost particle-size-independent. The deviations occur usually at the small particle sizes where pressure drops across the column are highest and irregular flow patterns are most likely.

TABLE V
Volume of Dye Treated at 50% Breakthrough for Different Chitin Particle Size Ranges

Dye	Chitin size range (μm)	Flow rate ($cm^3 \cdot min^{-1}$)	Volume treated (dm^3)
CI Acid Blue 25	710–1000	95	24
CI Acid Blue 25	255–355	96	18
CI Acid Blue 25	355–500	93	21
CI Acid Blue 25	500–710	93	24
CI Acid Blue 158	500–710	63	26
CI Acid Blue 158	150–250	65	35
CI Acid Blue 158	250–355	64	27
CI Acid Blue 158	355–500	64	25
CI Mordant Yellow 5	710–1000	80	16
CI Mordant Yellow 5	250–355	65	16
CI Mordant Yellow 5	355–500	84	17
CI Mordant Yellow 5	500–710	78	15
CI Direct Red 84	500–710	65	1.4
CI Direct Red 84	250–355	65	1.7

Nevertheless, the basic BDST eq. (5) is sufficient to represent the experimental data quite well.

CONCLUSION

The design procedures for batch and continuous fixed bed adsorption columns have been investigated for four dyestuffs on chitin. Batch adsorber design data are based on the Langmuir isotherm. Columnar operation indicates that chitin has a high capacity for CI Acid Blue 25, CI Acid Blue 158, and CI Mordant Yellow 5, but a low capacity for CI Direct Red 84. This low uptake is possible due to the fact that CI Direct Red 84 is a much larger dye molecule and cannot penetrate the internal pore structure of the chitin particle. The main fixed bed variables studied include bed height, dye flow rate, and chitin particle size, and these effects have been correlated with a simplifed design model, i.e., the bed depth service time model.

APPENDIX: NOMENCLATURE

a,a' constants in BDST equations
b constant in eq. (5)
B Langmuir constant ($dm^3 \cdot mg^{-1}$)
C_0 initial concentration of dye in solution ($mg \cdot dm^{-3}$)
C_1 final concentration of dye in solution ($mg \cdot dm^{-3}$)
C_∞ equilibrium concentration of dye in solution ($mg \cdot dm^{-3}$)
d arithmetic mean particle diameter (μm)
F dye flow rate ($dm^3 \cdot min^{-1}$)
G quantity of effluent to be treated (dm^3)
k_a rate constant for adsorption ($dm^3 \cdot min^{-1} \cdot mg^{-1}$)
K_L Langmuir equilibrium constant ($dm^3 \cdot mg^{-1}$)
L quantity of adsorbent (g)
L_b depth of adsorbent bed (cm)

n Freundlich exponent
N_0 adsorption capacity (mg·dm^{-3})
P Freundlich constant
t time (min)
u dye velocity (cm·min^{-1})
X_0 initial concentration of dye on chitin (mg·g^{-1})
X_1 final concentration of dye on chitin (mg·g^{-1})

Greek Symbols

ϕ BDST constant in eq. (10)

Subscripts

1,2 conditions at points 1 and 2

References

1. G. McKay, H. S. Blair, and J. R. Gardner, *J. Appl. Polym. Sci.*, **27**, 3043 (1982).
2. G. McKay, H. S. Blair, and J. R. Gardner, *J. Appl. Polym. Sci.*, **27**, 4251 (1982).
3. G. McKay, H. S. Blair, and J. R. Gardner, *J. Appl. Polym. Sci*, to appear.
4. G. S. Bohart and E. Q. Adams, *J. Chem. Soc.*, **42**, 523 (1920).
5. A. S. Michaels, *Ind. Eng. Chem.*, **44**, 1922 (1952).
6. M. Dole and I. M. Klotz, *Ind. Eng. Chem.*, **38**, 1289 (1946).
7. R. A. Davies, H. J. Kaempf, and M. M. Clemens, *Chem. Ind.* (Sep), 827 (1946).
8. R. A. Hutchins, *Chem. Eng.*, **80**, 133 (1975).

Received March 8, 1983
Accepted July 12, 1983
Corrected proofs received March 5, 1984